

Article

Purification of Andrographolide Methanolic Extract Using Molecularly Imprinted Polymer Prepared by Precipitation Polymerization

Wiwin Winingsih^{1,2} , Slamet Ibrahim¹ and Sophi Damayanti^{1,*}

¹ Pharmacochemistry Research Group, Bandung Institute of Technology, School of Pharmacy, Ganesha 10, Bandung 40132, Indonesia; wiwinwidaningsih@stfi.ac.id (W.W.); sibrahim@fa.itb.ac.id (S.I.)

² Sekolah Tinggi Farmasi Indonesia, Indonesian School of Pharmacy, Soekarno-Hatta No. 354, Bandung 40266, Indonesia

* Correspondence: sophi.damayanti@fa.itb.ac.id

Abstract: Molecularly Imprinted Polymer (MIP) has a specific cavity in which the conformity of shape, size, and functionalities corresponds with its template molecule and has been widely used in separation processes. Therefore, this study aims to examine the application of MIP for the purification of andrographolide. The MIP was synthesized by precipitation polymerization using methacrylic acid (MAA) and ethylene glycol dimethacrylate (EGDMA) as the functional monomer and cross-linker, andrographolide as a template, and acetonitrile:toluene (3:1) as porogen solvent. The results showed that the binding capacity of Synthesized MIP was 1.2486 mg/g, while the particle size was 295.5 nm with a polydispersity index of 0.064. Furthermore, the imprinting and selectivity factors were 1.148 and 12.37, respectively. The purification process by MIP increased the purity from 55.37 ± 0.69 to $94.94\% \pm 0.34$, while the isolate characterization showed that purified andrographolide had a similar character compared to the standard.

Keywords: andrographolide; molecularly imprinted polymer; precipitation polymerization



Citation: Winingsih, W.; Ibrahim, S.; Damayanti, S. Purification of Andrographolide Methanolic Extract Using Molecularly Imprinted Polymer Prepared by Precipitation Polymerization. *Sci. Pharm.* **2022**, *90*, 27. <https://doi.org/10.3390/scipharm90020027>

Academic Editor: Murali Mohan Yallapu

Received: 17 December 2021

Accepted: 13 April 2022

Published: 26 April 2022

Publisher's Note: MDPI stays neutral with regard to jurisdictional claims in published maps and institutional affiliations.



Copyright: © 2022 by the authors. Licensee MDPI, Basel, Switzerland. This article is an open access article distributed under the terms and conditions of the Creative Commons Attribution (CC BY) license (<https://creativecommons.org/licenses/by/4.0/>).

1. Introduction

Andrographolide (Figure 1) is a major bioactive constituent of *Andrographis paniculata* (*Acanthaceae*) and has been designated as a prospective pharmaceutical entity. This Labdane diterpenoid lactone in traditional Chinese medicine is used as an immunostimulant, as well as for dyspepsia, blood purification, asthma, gonorrhea, piles, dysentery, influenza, gastric complaints, fever, diarrhea, pharyngotonsillitis, snake bite, myocardial ischemia, common cold, diabetes, respiratory tract infections, and jaundice [1]. Due to its important pharmacological activity, various studies which aim to obtain andrographolide in high purity have been investigated. Several isolation methods involving numerous recrystallizations steps as purification methods have been reported [2–4]. However, the purification of crude andrographolide by MIP has not been carried out previously. Considering that MIP is widely used as a sorbent in separation methods such as solid-phase extraction (SPE), namely molecularly imprinted solid-phase extraction (MISPE) and chromatography, the use of MIP in the isolation purification step might simplify the process.

Molecularly imprinted polymers (MIP) are synthetic polymers characterized by selective cavities for certain groups of structurally related molecules [5]. It is synthesized by free radical polymerization and the sol-gel process. Bulk polymerization was the first free radical method used to prepare MIP, but it has several drawbacks, such as, requiring grinding and sieving as post-treatment leads to multiple binding sites, time-consuming, varying size and shape, as well as deeply embedded recognition sites which decrease the accessibility of target molecules. Other methods have been developed to overcome these drawbacks, namely suspension, precipitation, and polymerization in heterogeneous systems [6–10].

However, the utilization of emulsifiers in suspension and dispersion processes which are adsorbed on the surface particles, interferes with the desired target selective recognition and binding molecule. Therefore, the polymerization process without an attractive and suitable emulsifier was developed for generating MIP particles. Precipitation polymerization involves homogeneous nucleation in MIP particles formation. Initially, all components were mixed, while the critical chain lengths insoluble in the continuous phase were grown after polymerization to form particles and precipitate [7,11–16].

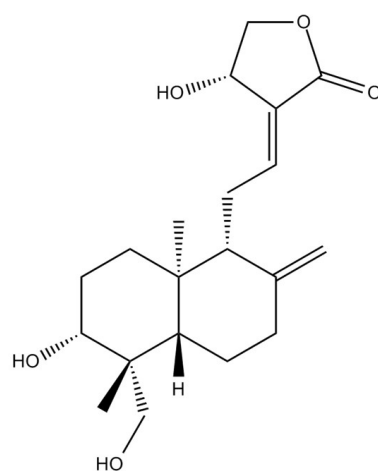


Figure 1. Structure of Andrographolide.

MIP has been used in several fields, such as drug delivery with specific targets [16–20], separation of related molecules and food adulterants in chromatography, industrial safety, and environmental analysis or separation [16,21,22]. It is also employed in the purification of biological, chemical reagents, and natural products [16,23–27]; therefore, in this study, MIP prepared using andrographolide as a template molecule was used for the purification. The application of MIP in the andrographolide isolation process is expected to speed up the purification process that was previously carried out by recrystallization, which usually takes days.

2. Materials and Methods

2.1. Materials

The materials used in this study were andrographolide standard (Tokyo Chemical Industry, Tokyo, Japan), EGDMA and MAA (Sigma Aldrich, St. Louis, MO, USA), Benzoyl peroxide, Methanol pro-HPLC (Fulltime, Anqing, China), Water pro-HPLC (Merck, Darmstadt, Germany), Toluene (Merck, Darmstadt, Germany), Acetonitrile pro-HPLC (Merck, Darmstadt, Germany), while andrographolide crude with 55.37% purity was made in our laboratory. Moreover, the characterization of materials and isolates was performed by FTIR (Thermo Scientific Nicolet iS5 ATR -ZnSe, Thermo Fisher Scientific, Waltham, MA, USA), SEM (Hitachi SU 3500, Hitachi, Tokyo, Japan), particle size analyzer (Horiba Scientific SZ—10, Horiba Scientific, Piscataway, NJ, USA), melting point apparatus (STUART, Cole - Palmer, Staffordshire, ST15 OSA, UK), and HPLC (Waters, 1525, Waters Corporation, Millford, MA, USA). The software used in this study was Gaussian 09 W version 8.0 and Gauss view 5.0. (Gaussian Inc., Wallingford, CT, USA; licence owned by Sekolah Farmasi Bandung Institute of Thechonoly)

2.1.1. Synthesis of Molecularly Imprinted Polymer (MIP)

MIP was synthesized by the precipitation polymerization method adopted by Krishnan et al. [23]. A measure of 0.3 mmol andrographolide and 0.9 mmol methacrylic acid (MAA) were dissolved in 50 mL of acetonitrile with a toluene mixture of 3:1 and sonicated for 5 min 6 mmol of ethylene glycol dimethacrylate (EGDMA) and 20 mg of benzoyl per-

oxide were then added to the mixture and sonicated for 40 min. The final mixture was sealed and placed in the oven at 70 °C for 24 h. In contrast, non-MIP (NIP) was synthesized similarly without andrographolide addition; after 24 h, the precipitate was separated by centrifugation at 4000 rpm for 40 min. MIP was sonicated with methanol: acetic acid (9:1 *v/v*) to remove the template, followed by methanol and water to remove another reagent. The process was repeated until there were no andrographolide peaks in spectrophotometry UV-Vis spectrum and HPLC chromatogram. Then, the synthesized polymer was dried at 60 °C for 16 h.

2.1.2. Surface Morphology Characterization with Scanning Electron Microscopes (SEM)

The surface morphology of MIP and NIP was assessed using SEM, and the sample to be analyzed was placed on a double side metal plate and then gold-plated under vacuum. The scanning process was carried out with a current of 60 mA and electric power of 15 V.

2.1.3. Determination of Particle Size and Polydispersity Index (PI)

Determination of particle size and PI were carried out by dispersing a 0.25 mg sample in 5 mL of water and inserted into the PSA instrument at a temperature of 25 °C.

2.1.4. Characterization of MIP and NIP by Fourier Transform Infrared (FTIR)

The synthesized polymer was characterized using FTIR ATR Zn-Se at a wave number of 400–4000 cm^{-1} . Then, the MIP and NIP FTIR spectrums were compared with the spectrum of constituent components.

2.1.5. Isotherm Adsorption Evaluation

Then, 20 mg of polymer were shaken with 5 mL of various concentrations ranging from 20–60 ppm andrographolide solution for 3 h and was left for 24 h. The residue and filtrate were separated by centrifugation at 4000 rpm for 40 min, while HPLC was used to determine the concentration of andrographolide left in the solution. The data were used to obtain the fit model of Freundlich, Langmuir, Temkin, and Henry.

2.1.6. MIP and NIP Performance Evaluation

The performance of MIP and NIP were evaluated by determining the imprinting and selectivity factors calculated by Equations (2) and (3). Quercetin was chosen as a comparison compound for determining the selectivity factor, which was evaluated by comparing the imprinting factor of MIP to that of andrographolide and quercetin [10,24–26].

$$KD = \frac{(C_i - C_f)V}{C_f W} \quad (1)$$

$$IF = \frac{KDMIP}{KDNIP} \quad (2)$$

$$\alpha = \frac{IF \text{ MIP andro}}{IFMIP \text{ quer}} \quad (3)$$

where KD is the distribution coefficient, C_i and C_f (mg/L) are concentrations of andrographolide before and after adsorption experiments, W (g) is the weight of the polymer, while V (L) is the volume of andrographolide solution. Furthermore, IF stands for imprinting factor, KD MIP and NIP represent the distribution coefficient of MIP and NIP, respectively. IF MIP andrographolide is the imprinting factor of MIP to andrographolide, while IF MIPquer represents that of MIP to quercetin.

2.1.7. Reuse Ability Test

The reuse ability of MIP was evaluated by treating it with several isotherm adsorption cycles and template removal cycles with methanol:water (9:1). The adsorption capacity of MIP and NIP at each cycle was determined and tabulated into a graph.

2.1.8. Purification of Andrographolide Methanolic Extract

The procedure of purification andrographolide methanolic extract was as follows, a 5 g extract, 100 mL methanol, and 5 g of MIP were shaken at 240 rpm for 2 h, and then separated by centrifugation. The residue was washed with hot water and cold methanol, then separated by centrifugation, while 25 mL of methanol at room temperature was used to wash the residue 3 times. After centrifugation, the filtrate was evaporated, and the white crystal of andrographolide isolate was collected for further characterization. The purity of purified andrographolide was calculated by Equation (4). Further, purified andrographolide was characterized by FTIR, Spectro-photometry UV-Vis, melting point, and HPLC.

$$\% \text{ purity} = \frac{\text{AUC sample}}{\text{AUC standard}} \times \frac{1}{\text{standard purity}} \times \frac{\text{C standard}}{\text{C sample}} \times 100\% \quad (4)$$

AUC was area under curve, while C (mg/L) is the concentration of sample and standard.

3. Results and Discussion

3.1. Synthesis of MIP and NIP

MIP can be synthesized by free radical polymerization and the sol-gel process. This study synthesized MIP and NIP by the precipitation polymerization method, which is the most common and widely used. The precipitation polymerization method has advantages over the simple bulk polymerization method, namely, a spherical and uniform size [12,15]. It is advantageous if the sorbent is in the stationary phase for chromatography or SPE. Spherical and monodisperse particle shapes will produce a good separation profile. In addition, precipitation polymerization can prevent the destruction of particles due to grinding and filtering, which is usually performed in bulk polymerization [13]. This method begins with a homogenous system that becomes heterogeneous in the continuous phase. Initially, all components are completely soluble, but the polymer becomes insoluble and precipitates during initiation [28–32]. The interaction of andrographolide with MAA is depicted in Figure 2, while the scheme of reaction is shown in Figure 3.

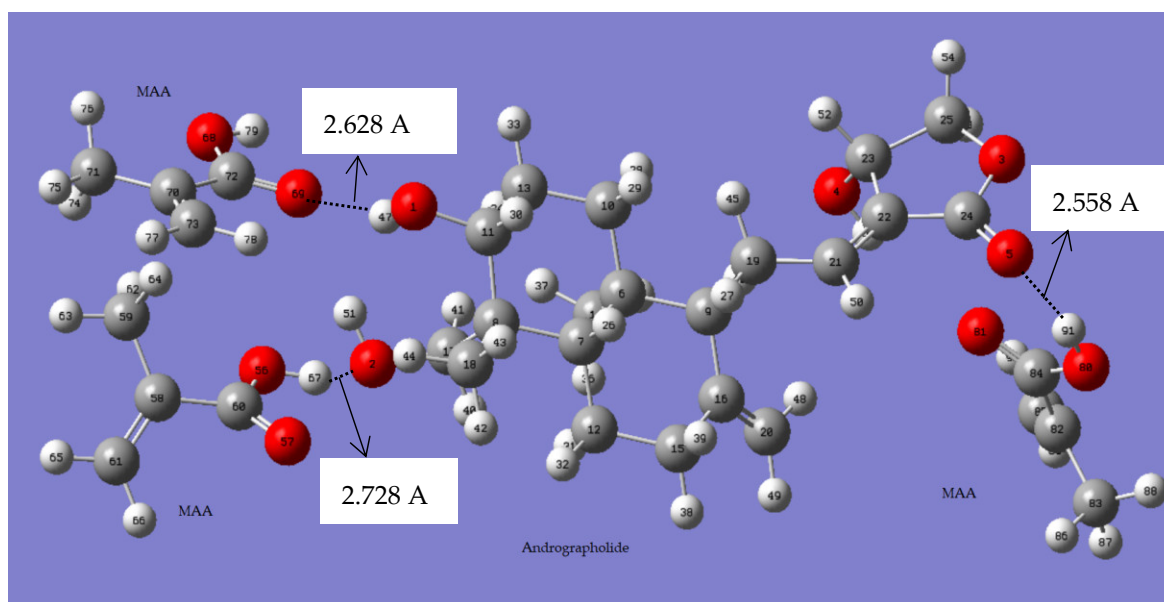


Figure 2. Predicted interaction between andrographolide and MAA (performed by Gaussian W 09).

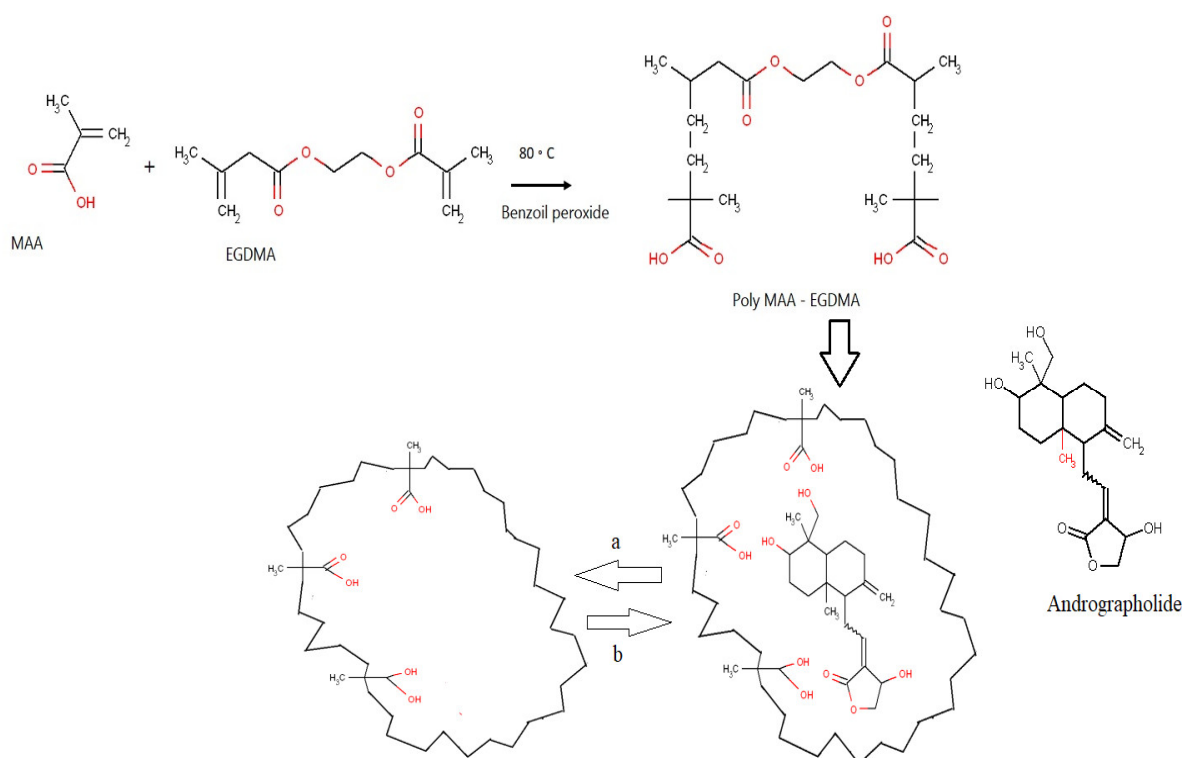


Figure 3. Proposed scheme of reaction of MIP synthesis; a: extraction of template molecule; b: rebinding of template molecule.

3.2. Characterization of MIP and NIP by SEM

SEM analysis is an important morphological study for polymer particles that provides an idea about the shape and size. Figure 4 indicates that spherical particles are produced with the size of nanometers. This is because the polymer particles were synthesized by precipitation polymerization. According to Tamayo et al., the uniform size of imprinted polymers can be formed using a noncovalent imprinting approach by precipitation polymerization [33,34].

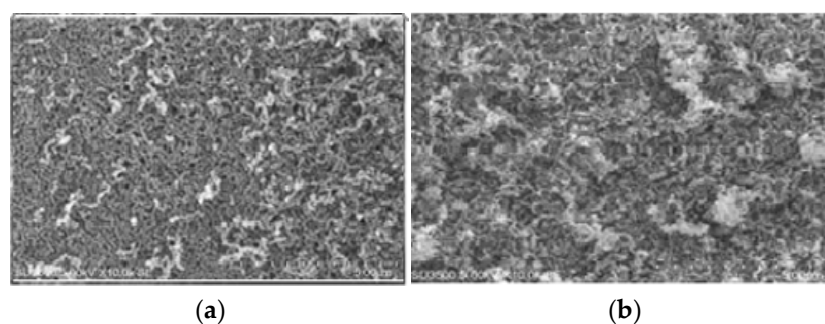


Figure 4. Surface morphology of MIP (a) and NIP (b).

3.3. Determination of Particle Size and Polydispersity Index

The result of particle size determination is shown in Table 1. MIP had a smaller size than NIP. It can be caused by the presence of a template molecule in MIP, which influences MIP particle growth in the polymerization step [35–37]. This evaluation also provided size distribution data of MIP and NIP, which is depicted in Figure 5. From this figure, we could find out that MIP had wider size distribution than NIP.

Table 1. Particle size and polydispersity index of MIP and NIP.

| Sample | Particle Size (nm) | Polydispersity Index |
|--------|--------------------|----------------------|
| MIP | 295.5 | 0.064 |
| NIP | 450.4 | 0.222 |

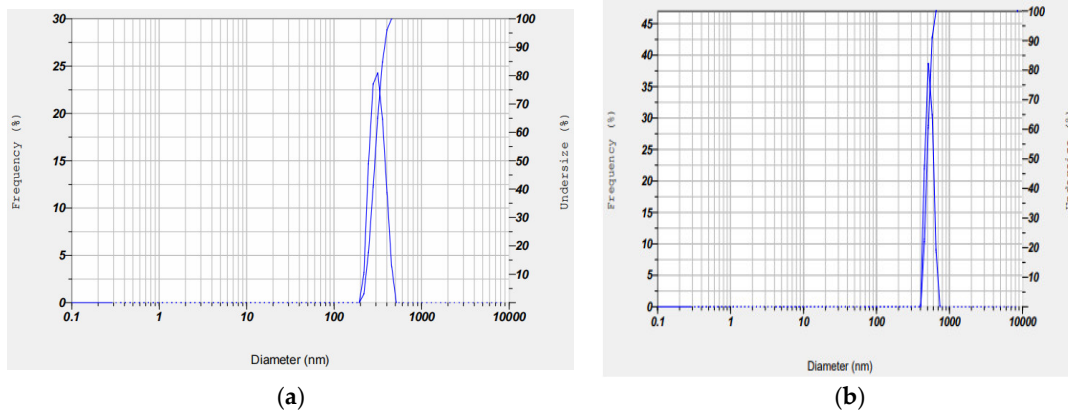


Figure 5. The size distribution curve of MIP (a) and NIP (b).

3.4. Characterization MIP and NIP by FTIR

FTIR cannot be used for confirmation of hydrogen interactions between templates and functional monomers. It is also stated by other researchers, such as Hasanah, 2019 [35], Zhi, 2018 [38]. FTIR MIP and NIP characterization with FTIR was used to determine the functional group present in the polymer. The FTIR spectrum provided information about changes in the functional group of the components before and after the synthesis process. A spectrum of EGDMA (cross-linker) and MAA (methacrylic acid) differed from MIP and NIP. The disappearance of the peak at about 1600 cm^{-1} , $1600\text{--}1635\text{ cm}^{-1}$, $990 \pm 5\text{ cm}^{-1}$, and $910 \pm 5\text{ cm}^{-1}$ due to the cleavage of the double bond during the polymerization process indicated the success of the synthesis process. Figure 6 shows the functional group of MIP and NIP compared to the monomer and cross-linker.

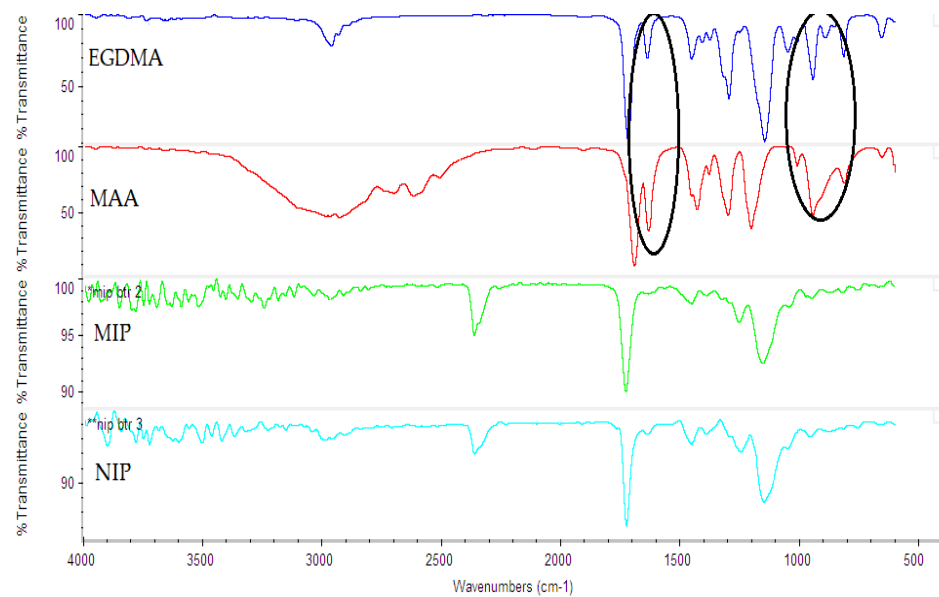


Figure 6. FTIR spectrum of MIP and NIP compared to EGDMA (cross-linker) and MAA (functional monomer).

3.5. Isotherm Adsorption Evaluation

Based on the isotherm graph, several adsorption isotherm parameters were determined, as shown in Table 2. Due to the selective cavity for andrographolide, the adsorption capacity of MIP (1.2486 mg/g) was bigger than NIP (0.1681 mg/g). Meanwhile, the RL values of both MIP and NIP ranging from $0 < RL < 1$ was an indication that the type of adsorption was the most preferred (favorable).

Table 2. Isotherm Adsorption parameters of MIP and NIP.

| Isotherm Adsorption Model | Parameters | Polymer | |
|---------------------------|----------------|---------|--------|
| | | MIP | NIP |
| Langmuir | Qm (mg/g) | 1.2486 | 0.1681 |
| | KL (L/mg) | 4.1462 | 8.4509 |
| | RL | 0.8599 | 0.7534 |
| | R ² | 0.9939 | 0.9929 |
| Freundlich | Kf (mg/g) | 1.6982 | 0.8784 |
| | 1/n | 0.5843 | 0.8235 |
| | n | 1.7114 | 1.2143 |
| | R ² | 0.9981 | 0.9902 |
| Temkin | Aγ (L/mg) | 0.623 | 0.2027 |
| | b | 2.2188 | 0.3376 |
| | B (J/mol) | 3.747 | 5.149 |
| | R ² | 0.9766 | 0.9382 |
| Henry | KHE | 0.3678 | 0.4922 |
| | R ² | 0.9929 | 0.9912 |

The adsorption intensity parameter obtained from the Freundlich isotherm describes the heterogeneity of the adsorption surface; the smaller the value of $1/n$, the higher the heterogeneity. Furthermore, the value of n , which ranges from 0 to 10, indicates the desired adsorption process. The calculation of n and $1/n$ parameters showed that the n value ranges from 0 to 10, while the $1/n$ value was lower than 1, which indicates that the adsorption process was successful and occurred on a heterogeneous surface [39,40].

The Temkin isotherm is used to determine the heat of absorption, which can describe the adsorption process. A positive B value indicates an exothermic process and based on the Temkin adsorption parameter calculation, all adsorbents have a positive B value; hence, the adsorption process that occurred was exothermic [39–41].

The correlation coefficient (R^2) is used to determine which isotherm model is suitable for the adsorbent. The model representing the adsorption isotherm of an adsorbent needs to have an R^2 value greater than 0.95. According to the values of R^2 Freundlich (chemical adsorption), the adsorption isotherm model was the most suitable to describe MIP [39–41]. Meanwhile, the Langmuir isotherm model was most suitable to describe the NIP adsorption and showed that the interaction between andrographolide and NIP was physical adsorption.

3.6. Imprinting Factor (IF) and Selectivity Factor (α) Determination

The imprinting and selectivity factors are used to determine the performance of MIP, where the greater the values, the better the performance. MIP showed good performance with an IF and selectivity factor of more than 1 [10]. Selectivity of MIP was higher than NIP due to the presence of a specific binding site to andrographolide. The result can be found in Table 3.

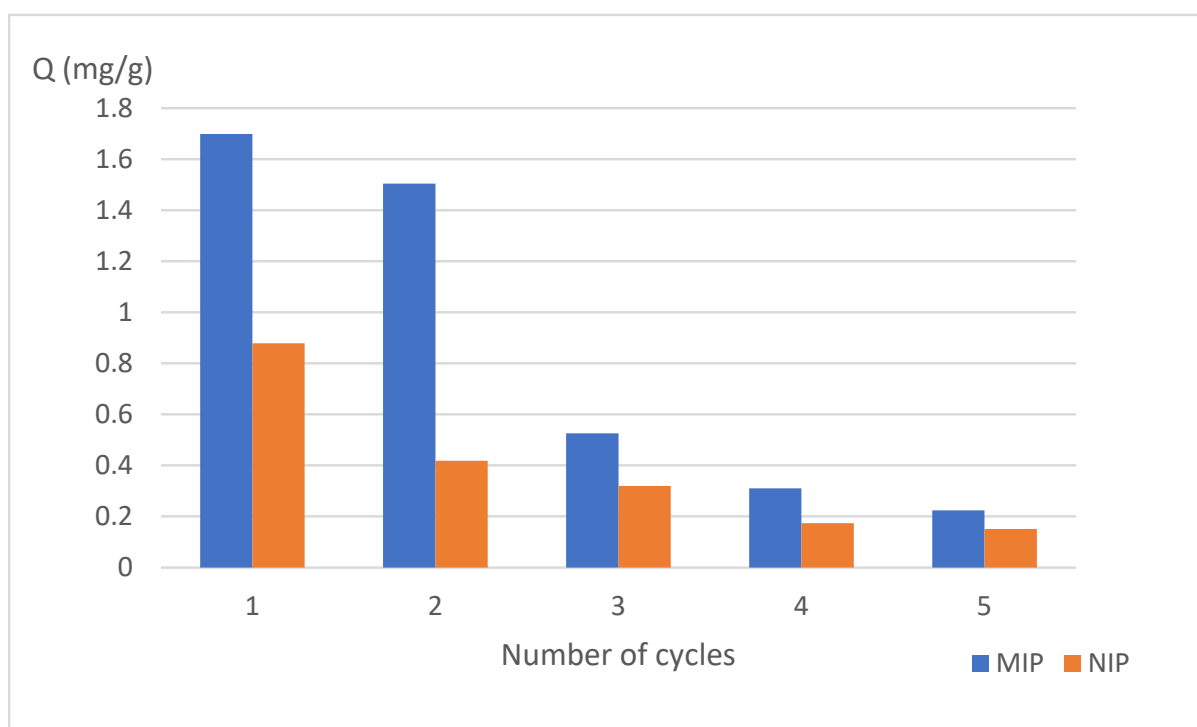
Table 3. Imprinting factor and selectivity factor of MIP and NIP.

| Polymer | KD _{andro} | KD _{quer} | IF _{andro} | IF _{quer} | α |
|---------|---------------------|--------------------|---------------------|--------------------|----------|
| MIP | 0.659 | 0.0102 | 1.148 | 0.0928 | 12.37 |
| NIP | 0.574 | 0.1094 | | | |

Note: KD_{andro}: distribution coefficient to andrographolide; KD_{quer}: distribution coefficient to quercetin; IF_{andro}: imprinting factor of polymer to andrographolide; IF_{quer}: imprinting factor of polymer to quercetin; α : selectivity factor.

3.7. Reuse Ability Test

The adsorption capacity of MIP decreased approximately 12% in the second cycle and significantly in the third to fifth cycles. The graph in Figure 7 shows that MIP could be used two times without significantly reducing the adsorption capacity. The significant decrease is presumably due to residual andrographolide, which still remains in the polymer (MIP and NIP) that can be observed in the FTIR spectrum of polymer before and after five cycles (Figure 8).

**Figure 7.** The adsorption capacity of MIP and NIP after undergoing five cycles isotherm adsorption studies.

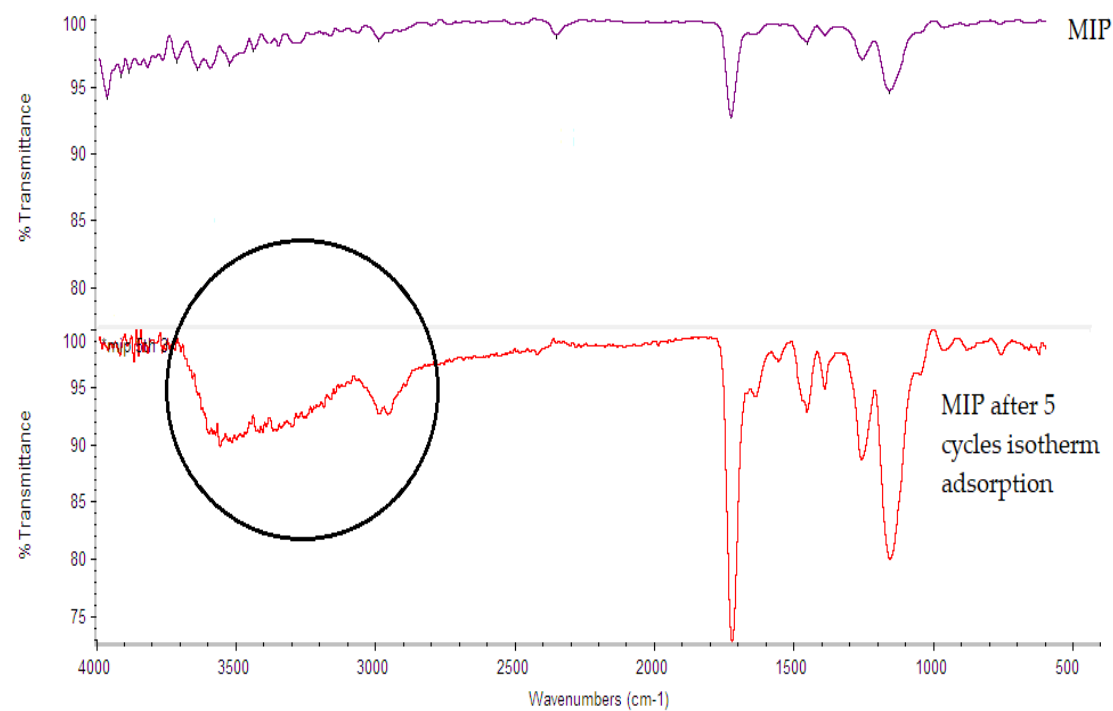
3.8. Application of MIP for Andrographolide Purification

The organoleptic appearance of andrographolide extract changed into a whiter color after a purification procedure with MIP (Figure 9). The color change indicates that MIP purification has improved the purity of the crude andrographolide.

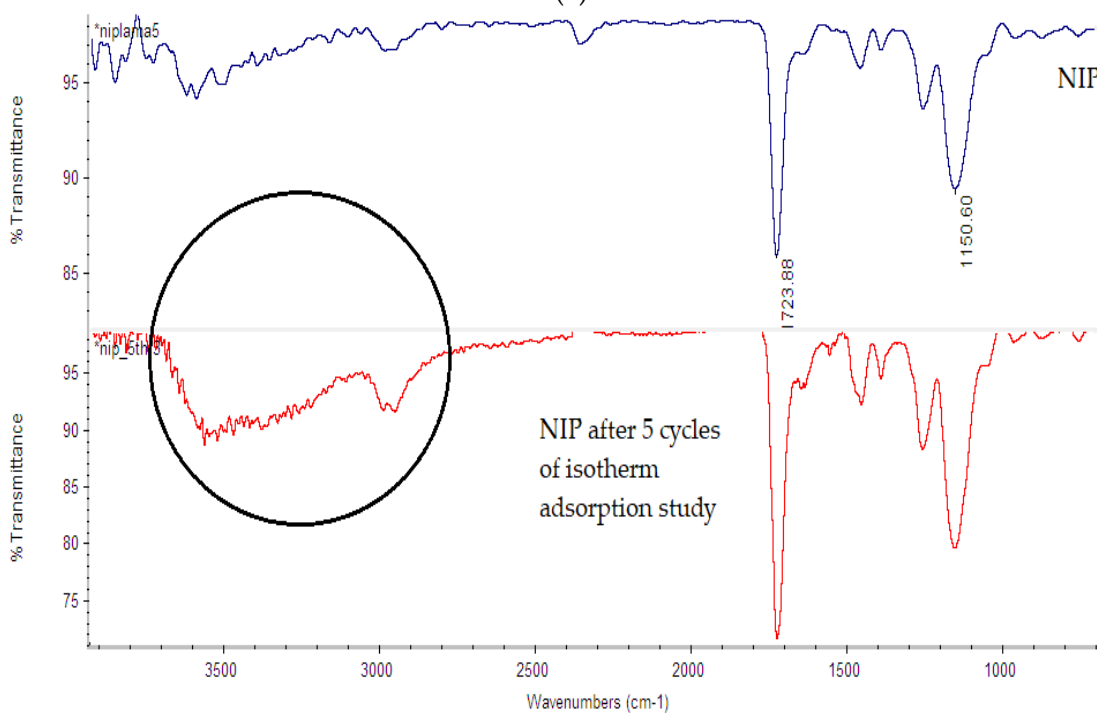
3.9. Characterization of Andrographolide Isolate

Andrographolide isolate was characterized by FTIR, spectrophotometry UV-Vis, HPLC, and melting point determination. The characterization method aims to confirm that the isolate obtained was andrographolide. The similarities in functional groups between standard andrographolide and isolate were determined using ATR-FTIR spectroscopy. The FTIR spectrum of the isolate showed characteristics of the lactone absorption band at 1722 cm⁻¹, C=C at 1674 cm⁻¹, C-O-C at 1218 cm⁻¹, and methylene at 906 cm⁻¹ (Figure 10). This absorption band was also detected in previous andrographolide IR spectrum studies [42]. The obtained ATR-FTIR spectrum showed close similarity between the transmittance sig-

nals of standard andrographolide and the isolate; therefore, the isolate was confirmed as andrographolide.



(a)



(b)

Figure 8. FTIR spectrum of MIP (a) and NIP (b) before and after undergo five cycles isotherm adsorption study.

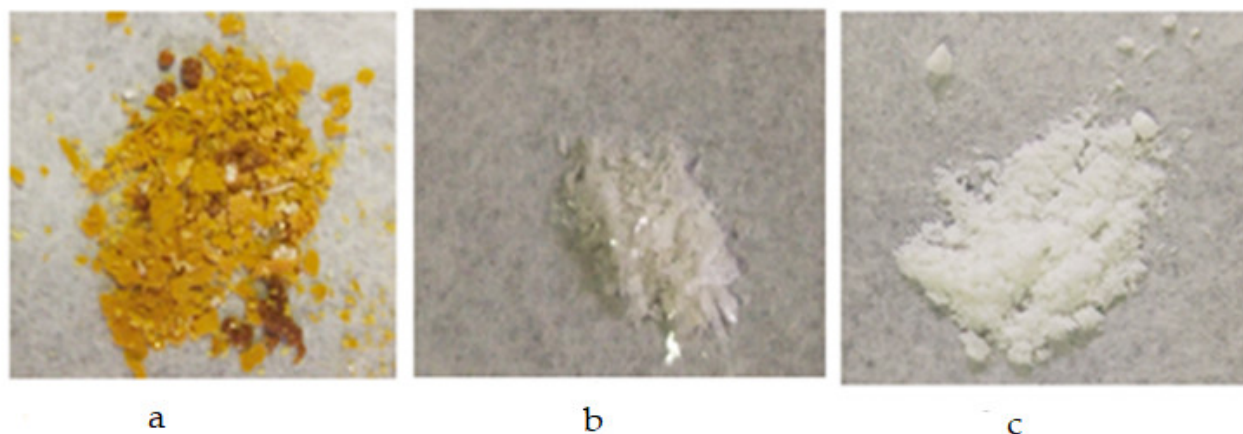


Figure 9. Organoleptic appearance of andrographolide extract (a), isolate after purification (b), and standard (c).

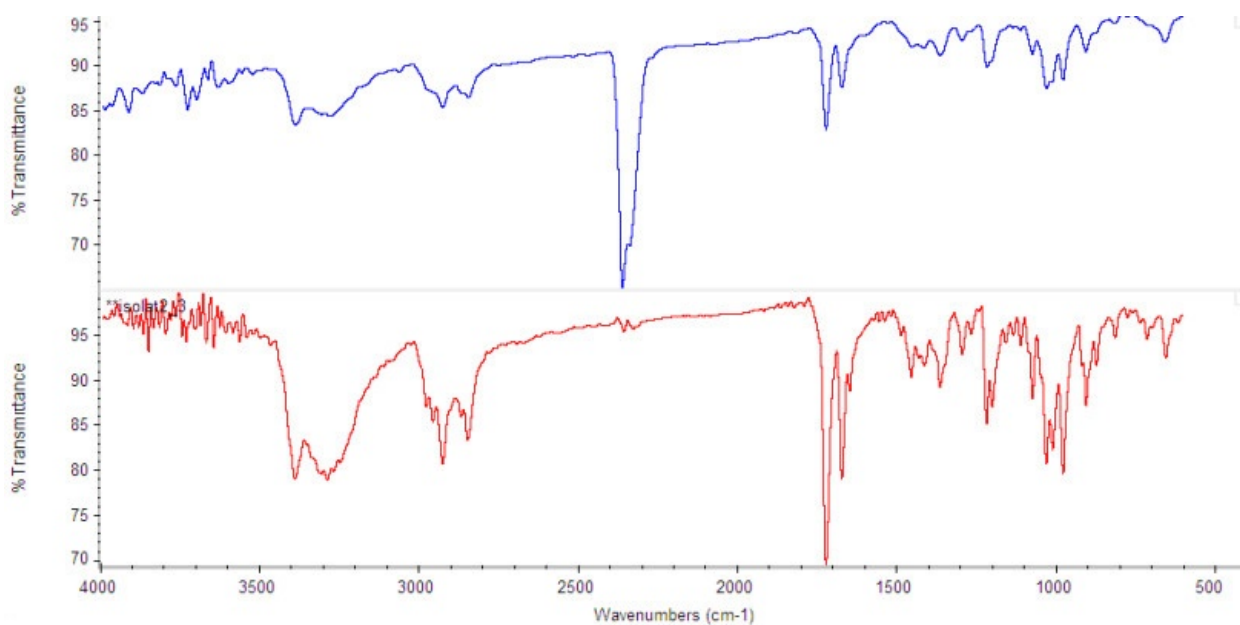


Figure 10. FTIR spectrum of andrographolide standard (blue) and isolate (red).

The HPLC method was used to examine the purity and confirm that the isolate was andrographolide by comparing the retention time with the standard. The chromatogram results showed the conformity of the isolate retention time with the standard (3.327 min). The isolate purity calculated by equation 4 was $94.94\% \pm 0.34$, while the purity of extract was $55.37\% \pm 0.69$. This result indicates that the purification of the extract sample with MIP had increased the purity. The chromatogram of the isolate, andrographolide standard, and crude is depicted in Figure 11.

Spectrophotometric UV-Vis was also used to evaluate the similarities between the isolate and standard spectrum. The result showed that the isolate had a similar spectrum pattern to the standard, as shown in Figure 12.

The melting point of the isolate was also determined and compared with the standard, and the result showed that the melting point of the standard was $228\text{ }^{\circ}\text{C}$, while that of the isolate was $229.8\text{ }^{\circ}\text{C}$. Additionally, the isolate characterization by FTIR, spectrophotometric UV-Vis, and melting point indicated similarity with the standard.

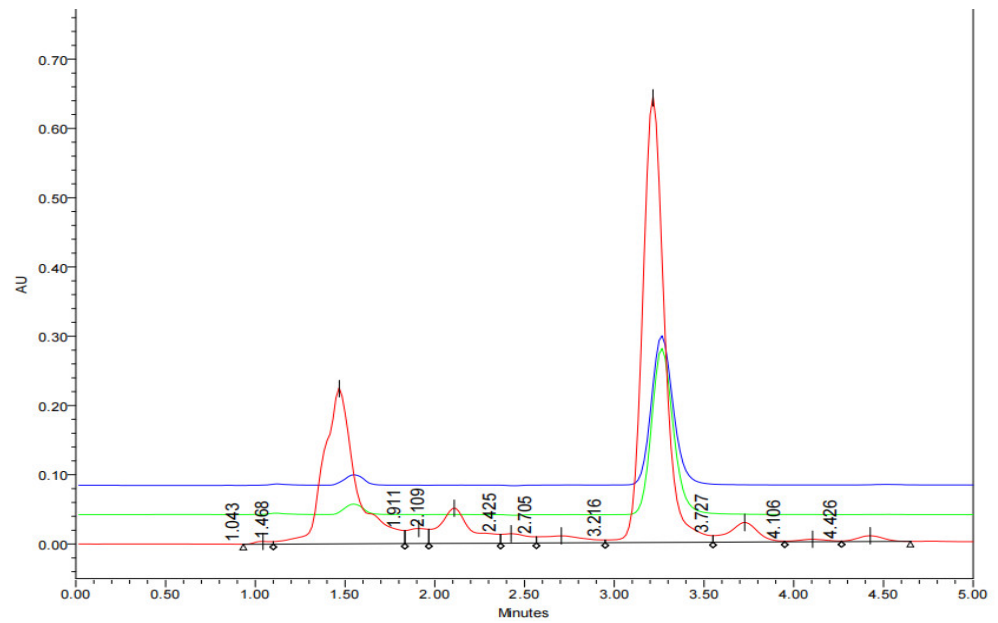


Figure 11. Chromatogram of andrographolide standard (green), isolate (blue), and andrographolide extract (red).

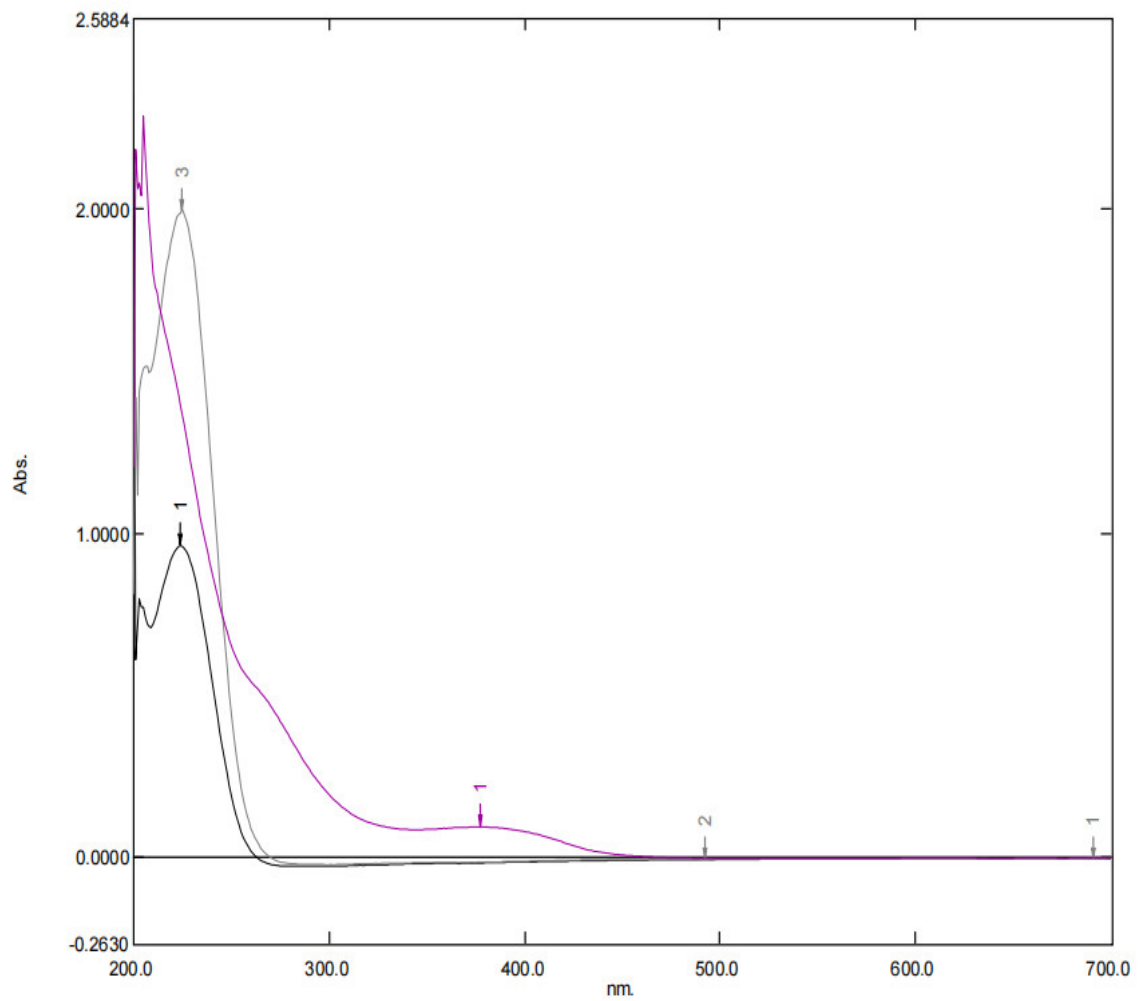


Figure 12. Spectrum UV-Vis of andrographolide extract (purple), isolate (grey), and standard (black).

4. Conclusions

Synthesized MIP has a spherical shape and smaller size compared to NIP, as well as better adsorption capacity, along with imprinting and selectivity factors. The application in the purification of andrographolide methanolic extract increased the purity, while the characterization of an isolate from this purification process showed similarity with the standard, indicating that MIP can be used to purify andrographolide.

Author Contributions: S.I. substantially contributed to the conception and design of the study, while W.W. participated in collecting and assembling data. S.I., S.D. and W.W. participated in processing analysis and interpretation of reported data, while W.W. contributed to the drafting of the article. Furthermore, S.I. and S.D. contributed to the critical revision on important intellectual content, while all authors read and approved the final manuscript before submission. All authors have read and agreed to the published version of the manuscript.

Funding: This research received financial support from P3MI Bandung Institute of Technology in 2019.

Institutional Review Board Statement: Not applicable.

Informed Consent Statement: Not applicable.

Data Availability Statement: All data generated during this study are included in the article.

Acknowledgments: We would like to appreciate P3MI Bandung Institute of Technology for the financial support.

Conflicts of Interest: The authors declare no conflict of interest.

References

1. Benoy, G.K.; Animesh, D.K.; Aninda, M.; Priyanka, D.K.; Sandip, H. An overview on andrographis paniculata (burm. F.) Nees. *Int. J. Ayurveda Res.* **2012**, *3*, 752–760. [CrossRef]
2. Liu, L.; Wencheng, Z.; Haitao, Z.; Ruixia, W.; Renjuan, Z. Method for Separating and Purifying Deoxyandrographolide. Available online: <https://patents.google.com/patent/CN101671320B/en?q=CN101671320B> (accessed on 14 September 2019).
3. Zhaokai, L.; Dongyang, X.; Depin, Z.; Huaxiang, L.; Shi, Y. Method for Extracting Andrographolidume from Andrographis Paniculata (Burm. F.) Nees. Available online: <https://patents.google.com/patent/CN105294618A/en?q=CN105294618A> (accessed on 10 January 2020).
4. Pundarikakshudu, K. A Simple and Facile Method for the Isolation of Andrographolide from Andrographis Paniculata Nees. *Am. J. PharmTech Res.* **2016**, *6*, 266–275.
5. Turiel, E.; Esteban, A.M. Molecularly imprinted polymers. In *Solid-Phase Extraction*; Elsevier: Amsterdam, The Netherlands, 2020; pp. 215–233.
6. Guo, L.J.; Qu, J.R.; Miao, S.S.; Geng, H.R.; Yang, H. Development of a molecularly imprinted polymer for prometryne clean-up in the environment. *J. Sep. Sci.* **2013**, *36*, 3911–3917. [CrossRef]
7. Karnka, R.; Chaiyasat, P.; Chaiyasat, A. Synthesis of Uniform and Stable Molecularly Imprinted Polymer Particles by Precipitation Polymerization. *Orient. J. Chem.* **2017**, *33*, 2370. [CrossRef]
8. Gong, X.Y.; Cao, X.J. Preparation of molecularly imprinted polymers for artemisinin based on the surfaces of silica gel. *J. Biotechnol.* **2011**, *53*, 8–14. [CrossRef] [PubMed]
9. Liu, J.; Deng, Q.; Tao, D.; Yang, K.; Zhang, L.; Liang, Z.; Zhang, Y. Preparation of protein imprinted materials by hierarchical imprinting techniques and application in selective depletion of albumin from human serum. *Sci. Rep.* **2014**, *4*, 1–6. [CrossRef]
10. Zhang, L.; Zhang, H.; Li, L.; Zuo, P.; Zhao, F.; Liu, M.; Ye, B.C.; Li, Y. Pneumocandin B 0 -imprinted polymer using surface-imprinting technique for efficient purification of crude product. *Anal. Sci.* **2016**, *32*, 923–930. [CrossRef]
11. Bakhtiar, S.; Bhawani, S.A.; Shafqat, S.R. Synthesis and characterization of molecular imprinting polymer for the removal of 2-phenylphenol from spiked blood serum and river water. *Chem. Biol. Technol. Agric.* **2019**, *6*, 1–10. [CrossRef]
12. Joke Chow, A.L.; Bhawani, S.A. Synthesis and characterization of molecular imprinting polymer microspheres of cinnamic acid: Extraction of cinnamic acid from spiked blood plasma. *Int. J. Polym. Sci.* **2016**, *2016*, 2418915. [CrossRef]
13. Fauziah, S.; Gafur, A.M.M.; Soekamto, N.H.; Taba, P.; Sapar, A. Synthesis and characterization of molecularly imprinted polymers of di-(2-Ethylhexyl) phthalate using the precipitation polymerization method. *Egypt. J. Chem.* **2021**, *64*, 2385–2392. [CrossRef]
14. Vasapollo, G.; Sole, R.; Del Mergola, L.; Lazzoi, M.R.; Scardino, A.; Scorrano, S.; Mele, G. Molecularly imprinted polymers: Present and future prospective. *Int. J. Mol. Sci.* **2011**, *12*, 5908–5945. [CrossRef] [PubMed]
15. Chen, L.; Wang, X.; Lu, W.; Wu, X.; Li, J. Molecular imprinting: Perspectives and applications. *Chem. Soc. Rev.* **2016**, *45*, 2137–2211. [CrossRef] [PubMed]
16. Belbruno, J.J. Molecularly Imprinted Polymers. *Chem. Rev.* **2019**, *119*, 94–119. [CrossRef] [PubMed]

17. Güney, O.; Serin, E. Stimuli-responsive molecularly imprinted hybrid polymer gel as a potential system for controlled release. *J. Appl. Polym. Sci.* **2016**, *133*, 42913. [[CrossRef](#)]
18. Lulinski, P. Molecularly imprinted polymers as the future drug delivery devices. *Acta Pol. Pharm.* **2013**, *70*, 601–609.
19. Luliński, P. Molecularly imprinted polymers based drug delivery devices: A way to application in modern pharmacotherapy. A review. *Mater. Sci. Eng. C* **2017**, *76*, 1344–1353. [[CrossRef](#)]
20. Suksuwan, A.; Lomlim, L.; Rungrotmongkol, T.; Nakpheng, T.; Dickert, F.L.; Suedee, R. The composite nanomaterials containing (R)-thalidomide-molecularly imprinted polymers as a recognition system for enantioselective-controlled release and targeted drug delivery. *J. Appl. Polym. Sci.* **2015**, *132*, 1–21. [[CrossRef](#)]
21. Anene, A.; Hosni, K.; Chevalier, Y.; Kalfat, R.; Hbaieb, S. Molecularly imprinted polymer for extraction of patulin in apple juice samples. *Food Control* **2016**, *70*, 90–95. [[CrossRef](#)]
22. Anirudhan, T.S.; Christa, J.; Deepa, J.R. Extraction of melamine from milk using a magnetic molecularly imprinted polymer. *Food Chem.* **2017**, *227*, 85–92. [[CrossRef](#)]
23. Li, Z.; Qin, C.; Li, D.; Hou, Y.; Li, S.; Sun, J. Molecularly imprinted polymer for specific extraction of hypericin from *Hypericum perforatum* L. herbal extract. *J. Pharm. Biomed.* **2014**, *98*, 210–220. [[CrossRef](#)]
24. Baker, Z.K.; Sardari, S. Molecularly Imprinted Polymer (MIP) Applications in Natural Product Studies Based on Medicinal Plant and Secondary Metabolite Analysis. *Iran. Biomed. J.* **2021**, *25*, 68. [[CrossRef](#)] [[PubMed](#)]
25. Jin, Y.; Row, K.H. Molecularly Imprinted Solid-Phase Extraction of Caffeine from Green Tea. *J. Ind. Eng. Chem.* **2006**, *12*, 494–499.
26. Ma, X.; Lin, H.; Zhang, J.; Zhou, X.; Han, J.; She, Y.; Rabah, T. Preparation and characterization of dummy molecularly imprinted polymers for separation and determination of farrerol from *Rhododendron aganniphum* using HPLC. *Green Chem. Lett. Rev.* **2018**, *11*, 513–522. [[CrossRef](#)]
27. Theodoridis, G.; Lasáková, M.; Škeříková, V.; Tegou, A.; Giantsiou, N.; Jandera, P. Molecular imprinting of natural flavonoid antioxidants: Application in solid-phase extraction for the sample pretreatment of natural products prior to HPLC analysis. *J. Sep. Sci.* **2006**, *29*, 2310–2321. [[CrossRef](#)]
28. Krishnan, H.; Islam, A.K.M.S.; Hamzah, Z.; Nadaraja, P.; Ahmad, M.N. A Novel Molecular Imprint Polymer Synthesis for Solid Phase Extraction of Andrographolide. *Indones. J. Chem.* **2019**, *19*, 219–230. [[CrossRef](#)]
29. Liu, H.; Zhou, Y.; Qi, Y.; Sun, Z.; Gong, B. Preparation of thiamphenicol magnetic surface molecularly imprinted polymers for its selective recognition of thiamphenicol in milk samples. *J. Liq. Chromatogr. Relat. Technol.* **2018**, *41*, 868–879. [[CrossRef](#)]
30. He, H.X.; Gan, Q.; Feng, C.G. An Ion-imprinted Silica Gel Polymer Prepared by Surface Imprinting Technique Combined with Aqueous Solution Polymerization for Selective Adsorption of Ni(II) from Aqueous Solution. *Chin. J. Polym. Sci.* **2018**, *36*, 462–471. [[CrossRef](#)]
31. Zhang, C.; Wang, Y.; Zhou, Y.; Guo, J.; Liu, Y. Silica-based surface molecular imprinting for recognition and separation of lysozymes. *Anal. Methods* **2014**, *6*, 8584–8591. [[CrossRef](#)]
32. Slomkowski, S.; Alemán, J.V.; Gilbert, R.G.; Hess, M.; Horie, K.; Jones, R.G.; Kubisa, P.; Meisel, I.; Mormann, W.; Penczek, S. Terminology of polymers and polymerization processes in dispersed systems (IUPAC Recommendations 2011). *Pure Appl. Chem.* **2011**, *83*, 2229–2259. [[CrossRef](#)]
33. Tamayo, F.G.; Casillas, J.L.; Martin-Esteban, A. Evaluation of new selective molecularly imprinted polymers prepared by precipitation polymerisation for the extraction of phenylurea herbicides. *J. Chromatogr. A* **2005**, *1069*, 173–181. [[CrossRef](#)]
34. Roland, R.M.; Bhawani, S.A. Synthesis and Characterization of Molecular Imprinting Polymer Microspheres of Piperine: Extraction of Piperine from Spiked Urine. *J. Anal. Methods Chem.* **2016**, *2016*, 5671507. [[CrossRef](#)] [[PubMed](#)]
35. Hasanah, A.N.; Dwi Utari, T.N.; Pratiwi, R. Synthesis of Atenolol-Imprinted Polymers with Methyl Methacrylate as Functional Monomer in Propanol Using Bulk and Precipitation Polymerization Method. *J. Anal. Methods Chem.* **2019**, *2019*, 9853620. [[CrossRef](#)] [[PubMed](#)]
36. Yoshimatsu, K.; Reimhult, K.; Krozer, A.; Mosbach, K.; Sode, K.; Ye, L. Uniform molecularly imprinted microspheres and nanoparticles prepared by precipitation polymerization: The control of particle size suitable for different analytical applications. *Anal. Chim. Acta.* **2007**, *584*, 112–121. [[CrossRef](#)] [[PubMed](#)]
37. Orowitz, T.E.; Ana Sombo, P.P.; Rahayu, D.; Hasanah, A.N. Microsphere polymers in molecular imprinting: Current and future perspectives. *Molecules* **2020**, *25*, 3256. [[CrossRef](#)] [[PubMed](#)]
38. Zhi, K.; Wang, L.; Zhang, Y.; Jiang, Y.; Zhang, L.; Yasin, A. Influence of size and shape of silica supports on the sol-gel surface molecularly imprinted polymers for selective adsorption of gossypol. *Materials* **2018**, *11*, 777. [[CrossRef](#)]
39. Edet, U.A.; Ifelebuegu, A.O. Kinetics, isotherms, and thermodynamic modeling of the adsorption of phosphates from model wastewater using recycled brick waste. *Processes* **2020**, *8*, 665. [[CrossRef](#)]
40. Boroumand Jazi, M.; Arshadi, M.; Amiri, M.J.; Gil, A. Kinetic and thermodynamic investigations of Pb(II) and Cd(II) adsorption on nanoscale organo-functionalized SiO₂Al₂O₃. *J. Colloid Interface Sci.* **2014**, *422*, 16–24. [[CrossRef](#)]
41. Singh, V.; Purohit, A.K.; Chinthakindi, S.; Goud, R.D.; Tak, V.; Pardasani, D.; Shrivastava, A.R.; Dubey, D.K. Analysis of chemical warfare agents in organic liquid samples with magnetic dispersive solid phase extraction and gas chromatography mass spectrometry for verification of the chemical weapons convention. *J. Chromatogr. A* **2016**, *1448*, 32–41. [[CrossRef](#)]
42. Indrati, O.; Martien, R.; Rohman, A.; Nugroho, A.K. Employment of ATR-FTIR and HPLC-UV method for detection and quantification of andrographolide. *Int. J. Appl. Pharm.* **2018**, *10*, 135–138. [[CrossRef](#)]